ARTICLE

Myopia-related stepwise and quadrant retinal microvascular alteration and its correlation with axial length

Mingming Liu[1] · Peng Wang[1] · Xiaojun Hu[1] · Chengcheng Zhu[1] · Ying Yuan[1] · Bilian Ke[1]

Abstract

Purpose To investigate the characteristics of retinal vascular alterations in patients with varying degrees of myopia, and to determine correlated variables and alteration patterns over different retinal zones.

Methods A total of 208 right eyes of 208 patients with myopia were enrolled and divided into mild, moderate, high, and extreme myopia groups. The macular vasculature in superficial, deep, and whole retinal layers was imaged with optical coherence tomography angiography (OCTA). The vessel densities over the whole annular zone, four quadrants, and six annuli were quantified as fractal dimension using a customized software. Simple linear regressions and ridge regression were used to determine and compare explanatory variables of microvascular density.

Results The microvascular density within the superficial, deep and whole retinal layers was highest in mild myopia group, second highest in moderate myopia group, second lowest in high myopia group and lowest in extreme myopia group. Within the same layer, differences between any two groups were significant (all $p < 0.05$). Among the four quadrants, only the inferior nasal (IN) quadrant showed no difference in microvascular density between mild and moderate groups. Ridge regression indicated that microvascular density values in all three layers were more strongly correlated with axial length (AL) (scaled estimates -0.139, -0.103, -0.154; all $p < 0.001$) than with spherical equivalent (SE) (scaled estimates -0.052, -0.096, -0.057; all $p < 0.05$).

Conclusions We characterized a stepwise and quadrant alteration of retinal microvascular density from mild to extreme myopia, which was more strongly affected by axial elongation, although both AL and SE were meaningful indicators.

Introduction

Myopia, which has a prevalence of 80–90% in Southeast Asia among young adults and is increasing in prevalence at an alarming rate worldwide [1, 2], is estimated to affect half of the global population by 2050 [3]. During the progression of myopia, axial length elongates along with ocular structural changes such as thinning of the retina and alteration of the retinal vasculature. Furthermore, this process may eventually lead to some vision-threatening diseases [4, 5]. Therefore, a considerable amount of research on myopia-related retinal vascular alterations has been carried out in the past few years [6–20].

Techniques such as fundus photography [6] and fluorescein angiography [7] have been used to investigate retinal vascular alterations. However, relatively low resolution and invasive procedures limited the application of the above techniques. Advances in some novel techniques such as optical coherence tomography angiography (OCTA) have enabled a more detailed exploration of retinal vasculature. OCTA is a noninvasive tool for three-dimensional visualization of retinal vasculature, which allows analysis over multiple retinal layers with high resolution. Its use has been widely expanding in clinical examinations as well as scientific investigations in various ocular diseases, including myopia [8–24]. Previous OCTA studies have reported decreased vascular density in myopia, especially high myopia [8–21]. Some research also suggested significant correlations between retinal vascular density and AL or SE [8, 9, 12, 13, 15, 17–20]. However, to our knowledge, retinal vascular alterations in mild-to-moderate and extreme

✉ Bilian Ke
  kebilian@126.com

[1] Institution: Department of Ophthalmology, Shanghai General Hospital, Shanghai Jiao Tong University School of Medicine, Shanghai, China

myopia groups are often overlooked and have not been thoroughly investigated yet. To the best of our knowledge, whether AL is a better indicator of myopia-related retinal microvascular alteration than SE has not yet been determined with statistical methods.

In this study, we stratified the subjects by the degree of myopic refractive error and aimed to characterize a more detailed pattern of retinal vasculature alterations in patients with different degrees of myopia with OCTA and our customized software. We also determined whether AL is a better indicator of retinal microvascular alterations than SE.

Methods

Study subjects

This research was conducted at Shanghai General Hospital. Two hundred and eight eligible myopic patients visiting our ophthalmology clinic were consecutively recruited between June 2017 and September 2018. All individuals underwent comprehensive ophthalmic examinations as follows: slit-lamp examination, ophthalmoscopic examination, best-corrected visual acuity (BCVA), axial length (AL), intraocular pressure (IOP), and refractive status. The inclusion criteria were as follows: refractive error $\leq -0.5D$; BCVA $\geq$ 0.8; and age from 18 to 45 years. The exclusion criteria were: a history of ocular trauma or surgery; a history of ocular and systemic diseases, including diabetes and hypertension; evidence of retinal pathology such as posterior staphyloma and chorioretinal atrophy; and use of medication that might affect the vasculature. Only data from right eyes were included for analysis. Informed consent was obtained from each recruited subject. This clinical study was conducted following the Declaration of Helsinki and approved by the Medical Ethics Committee of Shanghai General Hospital.

Axial length was obtained using an intraocular lens master (IOL master 500; Carl Zeiss Meditec), and the IOP was measured with an automatic non-contact tonometer (TX-F; Canon). Refractive error was presented in the form of SE, which was calculated as spherical dioptric power plus 1/2 cylindrical dioptric power. All ophthalmic parameters were measured three times by two skilled doctors independently, and the mean value was used. According to refractive status, the 208 right eyes were organized into four groups. Mild myopia group ($-3.0D <$ SE $\leq -0.5D$) consisted of 22 subjects; moderate myopia group ($-6.0D <$ SE $\leq -3.0D$) consisted of 72 subjects; high myopia group ($-10.0D <$ SE $\leq -6.0D$) consisted of 86 subjects; extreme myopia group (SE $\leq -10.0D$) consisted of 28 subjects.

Image acquisition and processing

After ophthalmic examinations, each participant underwent an OCTA scan of the $6 \times 6 \, mm^2$ angiograms centered on the fovea. All angiograms were obtained by the same proficient ophthalmologist using the same ZEISS Angioplex OCTA instrument (Zeiss Meditec, Inc., Dublin, CA, USA), which is capable of scanning at a rate of 68,000 A-scans per second and with a depth of 2 mm [25]. Angioplex OCTA is incorporated with tracking software known as FastTrac to minimize movement artifacts and speed up data acquisition [25]. The image acquisition process can be summarized with a three-step skeleton: scanning, algorithm, and imaging. First, two repeated B-scans were taken at the same position, each containing 350 A-scans equally spaced along the horizontal dimension and 350 B-scan positions in the vertical direction. Second, flow images were generated from repeated B-scans through an algorithm named OCT microangiography-complex (OMAG^c) [25]. Layer-by-layer visualization was realized through segmentation algorithms of the OCTA system such that superficial and deep layers were demarcated by the inner boundary of the inner nuclear layer (INL) [25]. To be more specific, the slab from the inner limiting membrane to the inner plexiform layer was defined as the superficial layer, and the slab from the INL to the outer plexiform layer refers to the deep layer. In the last step, images of superficial retinal layer, deep retinal layer, and whole retinal layer were exported.

The elongation of axial length in myopic eyes leads to a different magnification of OCTA images. Consequently, the application of magnification correction was needed to minimize errors caused by image distortion. Bennett's formula, using axial length as the primary correction factor [26], was clinically verified to be practical and to give a close approximation of the actual size of retinal features [27]. It has already been applied in several clinical investigations [8, 9, 28]. The relations between the real size (RS) and the captured picture size (CS) can be expressed as RS = CS $\times q^2$ (q represents the correction factor) and based on Bennett's method, $q = 3.382 \times 0.013062 \times (AL-1.82)$ [28]. Each image underwent adjustment according to the correction factor and was then resized to generate the corrected image with 1024×1024 pixels to meet the requirements of vessel segmentation (Fig. 1A–C).

Then the OCTA images were processed under the Matlab environment (The Mathworks, Inc., Natick, MA, USA). Microvascular networks (diameter < 25 μm) and macrovascular networks (diameter ≥ 25 μm) were separated by the customized segmentation algorithm through various steps, including inversion, equalization, background interference correction, and nonvascular structure elimination of images [29]. The deep macrovascular plexus was
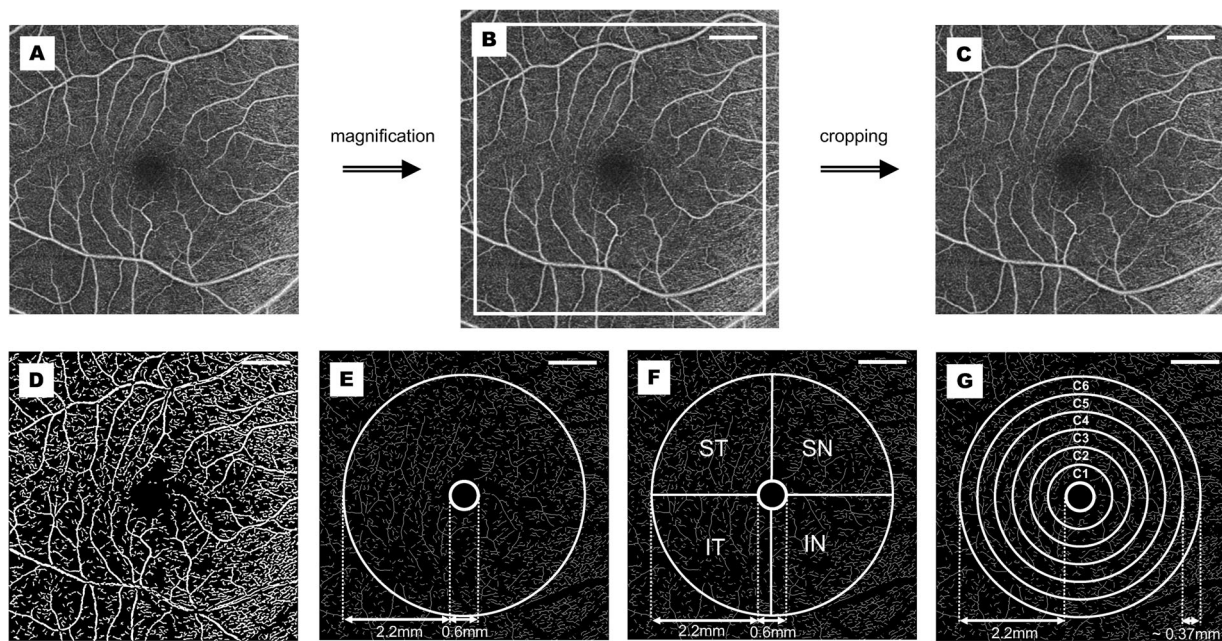
Fig. 1 Procedures of OCTA image processing. The original captured OCTA image (**A**) was magnified (**B**) according to Bennett's Formula, and then cropped into the original size (**C**) for following zoning and processing (**D–G**). A binary image was generated (**D**) after several procedures including inversion, equalization, background interference correction, and nonvascular structure elimination. After separation of macrovessels, the binary image was skeletonized (**E**), and the annular zone (without FAZ) with a bandwidth of 2.2 mm was demarcated for analysis (**E**). The whole annular zone was partitioned into four quadrants (**F**) and six annuli for regional analysis (**G**). OCTA optical coherence tomography angiography, FAZ foveal avascular zone, ST superior temporal, SN superior nasal, IN inferior nasal, IT inferior temporal. Scale bar = 1 mm.

under the potential influence of shadowgraphic artifacts from the superficial layer [30] and was therefore removed to reduce error. Then the binary images were skeletonized for further quantitative analysis through fractal analysis (box counting, D_{box}) (Fig. 1D, E). The fovea centralis was located by the software, and the foveal avascular zone (FAZ) was assumed to be the fovea-centered round area with a diameter of 0.6 mm. After the removal of the FAZ, the area from the boundary of the FAZ to the boundary of the fovea-centered 5 mm diameter circle was defined as the whole annular area. The whole annular area was equally divided into four parts by the horizontal and vertical line, and then the superior temporal (ST), superior nasal (SN), inferior nasal (IN), and inferior temporal (IT) quadrants were separately analyzed. Moreover, the software divided the whole annular zone into six annular zones centered at the fovea for annular analysis, each with a bandwidth of 0.37 mm (Fig. 1F, G).

Statistical analysis

Statistical analyses were performed with Statistical Package for Social Science software (SPSS, version 23.0, IBM Corp., Armonk, New York, USA) and R programming language (version 3.6.1). Results were presented in the form of the mean value ± standard deviation (SD). Chi-square tests were used to test gender differences and one-way analysis of variance (ANOVA) for age. One-way ANOVA was used to determine vascular density differences among four groups in the whole annular area, four quadrants, and six annular zones. Then post hoc multiple comparisons (LSD for data with equal variances and Dunnett's T3 for data with uneven variance) were performed to determine pairwise differences. Two-tailed Pearson's correlation test was used to determine the simple linear correlation between retinal microvascular density and independent factors. Variance inflation factor (VIF) was used to test the multi-collinearity of individual variables and ridge regression analysis (with R) was applied to obtain the optimal regression coefficients with the minimized influence of multicollinearity. Assessment of the images and data analysis were performed by investigators blinded to group allocation. Statistical significance was set as a *p* value below 0.05.

Results

Demographic characteristics

A total of 208 eyes of myopic patients were included in this research and stratified into four groups according to SE. The

Table 1 Clinical parameters and macular vascular density in different myopia groups.

	Mild ($n = 22$)	Moderate ($n = 72$)	High ($n = 86$)	Extreme ($n = 28$)	p value
Demographic and clinical parameters					
Gender, Male/Female	18/4	49/23	49/37	16/12	0.117
Age, Range, y	18–45	18–42	18–42	18–40	\
Age, Mean±SD, y	23.8 ± 8.4	23.5 ± 5.1	24.2 ± 5.6	25.9 ± 5.4	0.29
IOP, Mean±SD, mmHg	18.0 ± 2.4	17.6 ± 3.2	17.3 ± 2.7	17.5 ± 2.0	0.74
SE, Range, D	≤−0.5, >−3.0	≤−3.0, >−6.0	≤−6.0, >−10.0	≤−10.0	\
SE, Mean±SD, D	−2.24 ± 0.63	−4.78 ± 0.77	−7.60 ± 0.98	−12.40 ± 2.54	<0.001
AL, Range, mm	23.69–26.31	24.26–27.87	24.49–28.16	26.05–30.97	\
AL, Mean±SD, mm	24.92 ± 0.75	25.70 ± 0.83	26.65 + 0.85	28.41 ± 1.08	<0.001
Macular vascular density of whole annular zone					
Superficial microvessels	1.815 ± 0.010	1.806 ± 0.014	1.794 ± 0.023	1.776 ± 0.030	<0.001
Deep microvessels	1.802 ± 0.010	1.791 ± 0.015	1.783 ± 0.021	1.757 ± 0.035	<0.001
Retinal microvessels	1.812 ± 0.010	1.804 ± 0.015	1.791 ± 0.025	1.770 ± 0.033	<0.001
Superficial macrovessels	1.022 ± 0.017	1.017 ± 0.021	1.008 ± 0.022	1.009 ± 0.041	<0.001
Retinal macrovessels	1.012 ± 0.017	1.006 ± 0.022	0.997 ± 0.022	0.996 ± 0.033	<0.05
Microvasclar density of different quadrants					
Superficial ST	1.703 ± 0.015	1.696 ± 0.015	1.685 ± 0.023	1.670 ± 0.029	<0.001
Superficial SN	1.699 ± 0.014	1.689 ± 0.018	1.674 ± 0.029	1.655 ± 0.032	<0.001
Superficial IN	1.700 ± 0.014	1.700 ± 0.014	1.689 ± 0.021	1.670 ± 0.032	<0.001
Superficial IT	1.692 ± 0.013	1.681 ± 0.019	1.665 ± 0.030	1.642 ± 0.036	<0.001
Deep ST	1.686 ± 0.017	1.678 ± 0.019	1.671 ± 0.025	1.640 ± 0.049	<0.001
Deep SN	1.699 ± 0.013	1.684 ± 0.018	1.675 ± 0.025	1.659 ± 0.034	<0.001
Deep IN	1.683 ± 0.015	1.678 ± 0.022	1.669 ± 0.028	1.640 ± 0.046	<0.001
Deep IT	1.682 ± 0.012	1.669 ± 0.017	1.664 ± 0.025	1.640 ± 0.042	<0.001
Retinal ST	1.698 ± 0.013	1.694 ± 0.014	1.684 ± 0.023	1.666 ± 0.035	<0.001
Retinal SN	1.697 ± 0.013	1.688 ± 0.019	1.673 ± 0.030	1.651 ± 0.035	<0.001
Retinal IN	1.696 ± 0.014	1.697 ± 0.016	1.685 ± 0.024	1.660 ± 0.036	<0.001
Retinal SN	1.689 ± 0.015	1.676 ± 0.021	1.661 ± 0.033	1.637 ± 0.039	<0.001
Microvasclar density of different annuli					
Superficial C1	1.524 ± 0.042	1.505 ± 0.036	1.486 ± 0.063	1.429 ± 0.098	<0.001
Superficial C2	1.577 ± 0.022	1.564 ± 0.023	1.550 ± 0.039	1.517 ± 0.058	<0.001
Superficial C3	1.547 ± 0.012	1.536 ± 0.019	1.524 ± 0.030	1.497 ± 0.039	<0.001
Superficial C4	1.532 ± 0.013	1.523 ± 0.017	1.510 ± 0.026	1.489 ± 0.030	<0.001
Superficial C5	1.525 ± 0.014	1.517 ± 0.017	1.508 ± 0.021	1.489 ± 0.028	<0.001
Superficial C6	1.553 ± 0.011	1.545 ± 0.013	1.536 ± 0.020	1.523 ± 0.025	<0.001
Deep C1	1.360 ± 0.125	1.334 ± 0.102	1.311 ± 0.106	1.252 ± 0.137	<0.01
Deep C2	1.572 ± 0.015	1.558 ± 0.018	1.551 ± 0.035	1.515 ± 0.056	<0.001
Deep C3	1.538 ± 0.013	1.526 ± 0.019	1.521 ± 0.024	1.494 ± 0.039	<0.001
Deep C4	1.523 ± 0.014	1.511 ± 0.019	1.506 ± 0.023	1.482 ± 0.043	<0.001
Deep C5	1.516 ± 0.011	1.506 ± 0.016	1.499 ± 0.020	1.476 ± 0.035	<0.001
Deep C6	1.538 ± 0.013	1.529 ± 0.017	1.521 ± 0.020	1.500 ± 0.030	<0.001
Retinal C1	1.518 ± 0.034	1.498 ± 0.040	1.471 ± 0.068	1.415 ± 0.098	<0.001
Retinal C2	1.574 ± 0.023	1.566 ± 0.024	1.549 ± 0.042	1.511 ± 0.060	<0.001
Retinal C3	1.546 ± 0.011	1.536 ± 0.018	1.521 ± 0.031	1.490 ± 0.043	<0.001
Retinal C4	1.531 ± 0.012	1.520 ± 0.019	1.507 ± 0.028	1.482 ± 0.032	<0.001
Retinal C5	1.524 ± 0.015	1.514 ± 0.017	1.502 ± 0.023	1.482 ± 0.030	<0.001
Retinal C6	1.550 ± 0.008	1.542 ± 0.015	1.533 ± 0.021	1.517 ± 0.026	<0.001

The p values show the significance level of multi-group comparisons.

SD standard deviation, *IOP* intraocular pressure, *SE* spherical equivalent, *AL* axial length, *ST* superior temporal, *SN* superior nasal, *IN* inferior nasal, *IT* inferior temporal.

demographic and basic clinical parameters are presented in Table 1. Participants in different groups were age- and gender-matched (all $p > 0.05$). In addition, there was no significant difference in intraocular pressure (IOP, $p > 0.05$) among the four groups (Table 1).

Declining pattern of retinal microvascular density in patients with varying degrees of myopia

Compared to mild myopic eyes, the vascular density (represented with fractal dimension, D_{box}) of the microvasculature in

Fig. 2 Comparisons of whole annular micro- and macrovascular densities (D_{box}) among different myopic groups. Microvascular densities in superficial (**A**) and deep (**B**) layers showed a downward trend as myopia progressed (Mild > Moderate > High > Extreme), and the difference between adjacent groups was statistically significant as shown in the graphs. Microvascular and Macrovascular density in the whole retinal layer were shown in **C** and **D**. Macrovascular density in high myopia declined markedly in the whole retinal layers, but no statistical difference was found between moderate myopia and mild myopia. Statistical significance was marked as *($p \le 0.05$), **($p \le 0.01$), and ***($p \le 0.001$).
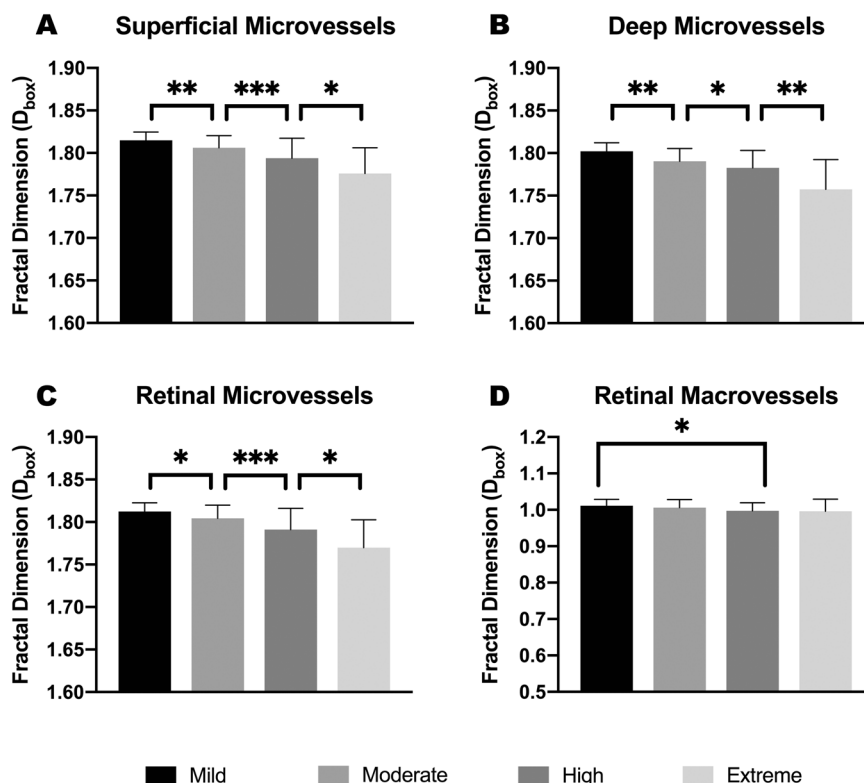
moderate myopia group was significantly reduced in the superficial ($p \le 0.01$), deep ($p = 0.01$) and whole ($p < 0.05$) retinal layers. Similarly, highly myopic eyes showed a significantly lower microvascular density than moderately myopic eyes ($p < 0.001$; $p < 0.05$; and $p < 0.001$, respectively), and extremely myopic eyes showed a significantly lower microvascular density than highly myopic eyes ($p < 0.05$; $p < 0.01$; and $p < 0.05$, respectively) in these three layers (Table 1 and Fig. 2). On the other hand, no significant differences were found between mild and moderate groups in either superficial or whole retinal layers when it comes to macrovascular density. The macrovascular density in high myopia was significantly reduced in comparison with mild group ($p < 0.05$) in the whole retinal layer, and was lower than mild ($p < 0.01$) and moderate ($p < 0.05$) groups in the superficial retinal layer (Table 1 and Fig. 2). As for extreme myopia, no reduction in the macrovascular density was observed in comparison with high myopia, in either the superficial ($p > 0.05$) or retinal ($p > 0.05$) layers.

Regional characteristics of microvascular alterations

In general, the microvascular density values over the four quadrants and six annular zones were lower in patients with myopia of a higher degree, except for the inferior nasal (IN) quadrants (Table 1 and Fig. 3). Compared to that in the mild myopia group, the inferior nasal microvascular density

within the superficial and whole retinal layers did not decrease in the moderate group (both $p = 1.000$) but decreased in the high and extreme myopia groups. Among the six annuli, we noticed a large standard deviation in the C1 annulus, which can be attributed to the individual variation and myopia-related alteration of FAZ [13, 31], and C1 was therefore excluded from further analysis. We calculated the magnitude of reduction as the difference in the fractal dimension between mild myopia and extreme myopia divided by the fractal dimension of mild myopia. The results showed a 2.15% reduction of the overall reduction magnitude within the superficial retinal, and the magnitudes were 3.82, 3.19, 2.77, 2.37 and 1.94% in C2–C6 annuli, respectively. For the deep retinal layer, the percentages of reduction were 2.47% in the whole annular zone and 3.62, 2.82, 2.72, 2.64 and 2.45% in C2–C6, respectively.

Correlations between AL and SE with microvascular density

Simple linear regression demonstrated negative correlations between AL and SE with microvascular density in the superficial ($r = -0.527$, $p < 0.001$; $r = -0.591$, $p < 0.001$), deep ($r = -0.573$, $p < 0.001$; $r = -0.576$, $p < 0.001$) and whole ($r = -0.526$, $p < 0.001$; $r = -0.597$, $p < 0.001$) retinal layers (Fig. 4). For macrovascular density, only a negligible negative correlation was found with SE and AL
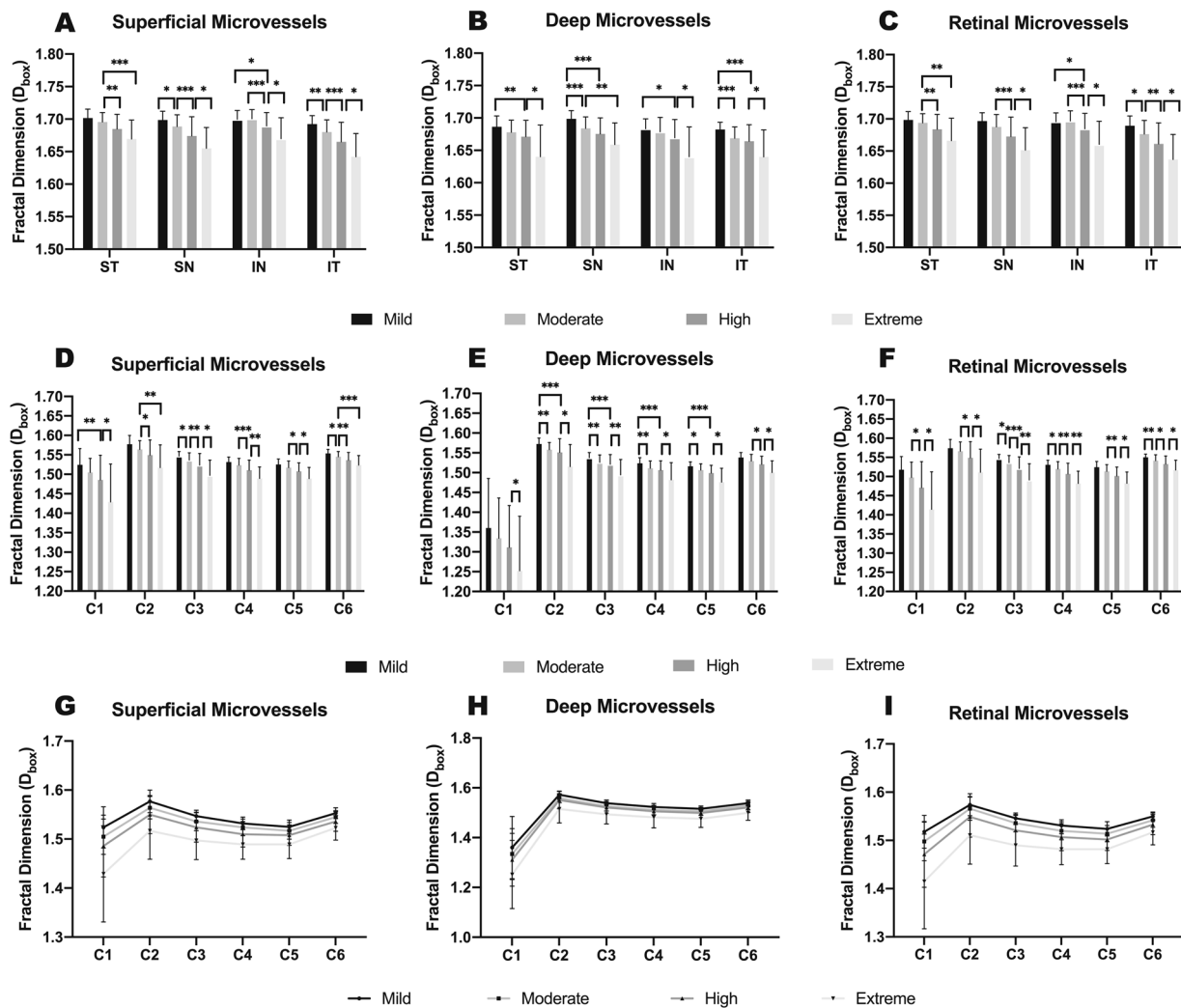
Fig. 3 Comparisons of microvascular densities (D_{box}) in four quadrantal zones and six annular zones in different myopic groups. For quadrantal partitions, superficial (**A**), deep (**B**), and whole (**C**) retinal layers generally presented lower microvascular densities in groups with lower SE, except for moderate myopia in IN zone. As myopia groups changed from mild to extreme myopia, microvascular densities decreased unevenly in 6 annular zones in all three layers (**D–F**). From C1 to C6, the gap between groups generally narrowed in all three layers (**G–I**). SE spherical equivalent, IN inferior nasal. Statistical significance was marked as *($p \leq 0.05$), **($p \leq 0.01$), and ***($p \leq 0.001$).

in the superficial ($r = -0.193$, $p < 0.01$; $r = -0.191$, $p < 0.01$) and whole retinal ($r = -0.211$, $p < 0.01$; $r = -0.163$, $p < 0.05$) layers. No correlations were found between IOP, age or sex and retinal vascular density (all $p > 0.05$). The correlation coefficient between AL and SE was 0.814, indicating multicollinearity of the two factors. Therefore, ridge regression analysis was applied to minimize the influence of multicollinearity and obtain optimal coefficients. Following multivariate ridge regression, AL and SE still showed significant correlation with microvascular density in superficial (scaled estimate -0.139, -0.052; $p < 0.001$, 0.031), deep (scaled estimate -0.103, -0.096; both $p < 0.001$) and whole (scaled estimate -0.154, -0.057; $p < 0.001$, 0.030) retinal layers.

Discussion

Retinal vascular alterations in myopia were extensively studied and were considered to be associated with many complications of myopia [4, 5, 15], which is of broad interest to researchers. However, many related details remain unclear. With OCTA as the main tool, this study described the step-by-step pattern of myopia-related retinal microvascular alterations and their quadrant differences. Based on continuous and wide ranges of SE (-0.5D to -19.0D) and AL (23.69 to 30.97 mm), we further determined that the retinal microvasculature was more sensitive to axial elongation than the increase in the diopter of myopia.
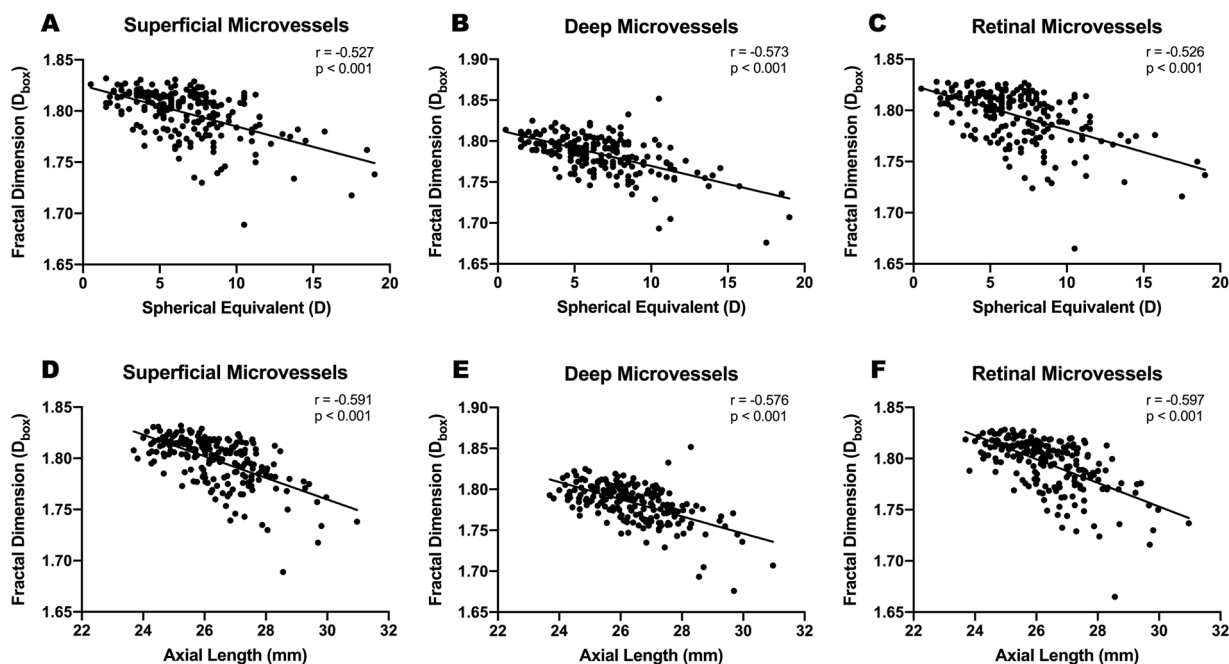
Fig. 4 Simple linear regression analysis between SE and AL with quadrantal microvascular densities (D_{box}) in all three layers. Microvascular density (D_{box}) showed negative correlations with the absolute value of spherical equivalent (**A–C**) and axial length (**D–F**) in all three layers. Pearson Correlation Coefficient (r) and p value were presented in corresponding graphs. SE spherical equivalent, AL axial length.

In the current study, we characterized an almost synchronous myopia-related retinal microvascular reduction in both the superficial and deep retinal layers, which occurred in a step-by-step declining pattern from the mild to extreme myopia groups. Our result was partially in accordance with several prior studies reporting loss of the retinal microvascular network in high myopia [6, 8–12, 32, 33]. However, unlike previous research, we mainly focused on alteration characteristics of various myopia groups by standardized myopia stratification, not merely high myopia. Our result suggested that the microvascular density was remarkably lower in moderate myopia than in the mild group and continued to decrease from high to extreme myopia. Myopia development is a continuous process of increase in the myopia diopter and elongation of axial length. Therefore, it can be reasonably speculated that during myopia progression, the retina is gradually stretched due to continuous elongation of the eyeball, resulting in a gradual decline in vascular density. Our result is supportive of this hypothesis, indicating alteration of retinal microvasculature in relatively lower degree of myopia. Therefore, great importance should be attached to the prevention and early intervention of myopia. On the other hand, we found that in contrast to the microvasculature, the macrovasculature was relatively unaffected in moderate myopia within the superficial and whole retinal layers, indicating its higher resistance to mechanical stretch and chemical stimulation. The different vulnerabilities between the macrovasculature and microvasculature were probably due to the structural differences in the vascular walls. The microvasculature is mainly composed of pericytes and endothelial cells, while the macrovascular wall is structurally thicker and contains more smooth muscle cells. In addition, based on the optical micro-angiography algorithm of OCTA, the vascular density is proportional to the flux rate of red blood cells passing through [34]. Thus, macrovessels should exhibit higher mechanical strength to resist internal and external stimuli, which instead makes microvascular density a more sensitive metric to evaluate vascular alteration.

For a more detailed insight into this stepwise microvascular alteration in myopia, we further divided the total annular zone into four quadrants and six annular zones to determine whether there are regional differences. Our statistical result suggested that myopia-related microvascular loss occurred in all four quadrants of the macular region in both the superficial and deep retinal layers, which, however, presented with regional preferences depending on the degree of myopia. In comparison to that in mild myopia, microvascular density in moderate myopia significantly decreased in the superior nasal and inferior temporal quadrants and slightly decreased in the superior temporal quadrant, but was not decreased in the inferior nasal sector. In high myopia, all quadrants showed significant decreases in comparison to the mild group. Thus, we speculated that the inferior nasal sector was the last affected quadrant in sequence, reflecting the relatively lower susceptibility of this quadrant. Using OCTA, Zhou and associates scanned an 8*8 mm^2 macular region

and found the largest blood flow area in the nasal region [35]. The abundant retinal vascular branches and sufficient basal blood flow in this region might be a plausible explanation for the relatively preserved inferior nasal vessels. Similarly, analysis of annular differences showed a general decline in microvascular density in all six annular zones. To explore the possible circular differences, we mainly compared the fractal dimension between extreme myopia and mild myopia. Over the whole annular zone, the microvascular density within the superficial retinal layer in extreme myopia displayed an ~2.35% reduction compared with that in mild myopia. The magnitudes of fractal dimension reduction were 3.82, 3.19, 2.77, 2.37 and 1.94% from C2 to C6, respectively. It seemed that the closer to the fovea, the more obvious the impact of mechanical stretch on the fractal dimension of retinal microvasculature. We surmised that a possible reason could be that the macular fovea has the thinnest retina in the posterior pole and a relatively thinner retina around it, making it more susceptible to mechanical stretch during axial elongation. Ohno-Matsui et al. [36] reported that ~88% of posterior staphyloma involved macula, reflecting the vulnerability of the macular region to mechanical stretch to some extent. However, the reduction in fractal dimension (no unit) does not completely equate to changes in retinal vascular density (unit %). The comparability between fractal dimension and microvascular density and the above hypothesis still need further validation.

Both AL and SE showed significant correlations with microvascular and macrovascular alterations in this study, but interestingly, AL showed a greater impact on retinal vascular density. Refractive status is determined by many refractive components of both the anterior and posterior segments of the eye, including corneal curvature, AL and so on. By contrast, axial elongation was generally considered to be the result of structural alterations in the posterior segment. In turn, axial elongation induced mechanical stretch and concomitant reduction of oxygen consumption will have an impact on the structures of the posterior segment, such as the retina [4, 37]. The natural deviation of corneal curvature and other refractive components in the healthy population are relatively limited, and AL progresses almost synchronously with SE during myopia development [38], making them both useful parameters for retinal vascular evaluation. However, they are not completely equivalent. To the best of our knowledge, AL and SE have not been compared directly in previous OCTA-based studies, possibly owing to the multicollinearity of the two parameters. In this study, we performed ridge regression to overcome the problem of multicollinearity and found that microvascular density correlated more strongly with AL than with SE. Therefore, in clinical practice, ophthalmologists and myopic patients might need to pay more attention to axial elongation rather

than only refractive status. In addition, we found no correlations between microvascular density and age in the present study, which was not consistent with the conclusion of Wei et al [39]. The likely reason for this inconsistency is the different age range of the studied population. Their participants were a population aged from 18 to 82 years, and their multigroup comparison indicated that only those aged 65 years or above showed a significant decrease in microvascular density. By contrast, our study excluded pathologic myopia and only encompassed an age range from 18 to 45 years, suggesting that in this age range, retinal vascular density was relatively unaffected by age.

Several limitations of this study should be noted. First, it is a cross-sectional research from hospital-based data, which thereby limits our ability to infer causality and determine the retinal vasculature alterations during the progression of myopia. Therefore, our findings need further validation through longitudinal studies. Second, the sample sizes in mild and extreme myopia groups were relatively small. However, we performed sample size calculation with G*power (version 3.1.9) [40] and found that our sample size was adequate to provide a detection power over 95%.

In conclusion, we found that the decrease of microvascular density may happen in the moderate myopia and continue its downtrend along with the deepening of myopia. The axial elongation-associated stepwise and quadrant retinal microvascular alterations in varying degrees of myopia indicate that microvascular density may serve as a promising indicator and be useful for understanding the underlying pathophysiological mechanism during myopia progression.

Summary

What was known before

1. Previous studies reported significant vascular density decrease in myopia, especially in high myopia.
2. The reduction of retinal vascular was correlated with axial length, spherical equivalent, and some other parameters.

What this study adds

1. We characterized a stepwise fashion of macular microvascular density reduction from mild to extreme myopia within both superficial and deep retinal layers.
2. This stepwise alteration showed regional susceptibilities over four quadrants and six annuli.
3. Retinal microvascular density was more strongly affected by axial elongation, although both axial length and spherical equivalent were meaningful indicators.

Compliance with ethical standards

Conflict of interest The authors declare that they have no conflict of interest.

Publisher's note Springer Nature remains neutral with regard to jurisdictional claims in published maps and institutional affiliations.

References

1. Morgan IG, French AN, Ashby RS, Guo X, Ding X, He M, et al. The epidemics of myopia: aetiology and prevention. Prog Retinal Eye Res. 2018;62:134–49.
2. Morgan IG, He M, Rose KA. EPIDEMIC OF PATHOLOGIC MYOPIA: what can laboratory studies and epidemiology tell us? Retina. 2017;37:989–97.
3. Holden BA, Fricke TR, Wilson DA, Jong M, Naidoo KS, Sankaridurg P, et al. Global prevalence of myopia and high myopia and temporal trends from 2000 through 2050. Ophthalmology. 2016;123:1036–42.
4. La Spina C, Corvi F, Bandello F, Querques G. Static characteristics and dynamic functionality of retinal vessels in longer eyes with or without pathologic myopia. Graefe's Arch Clin Exp Ophthalmol = Albrecht von Graefes Arch fur klinische und experimentelle Ophthalmologie. 2016;254:827–34.
5. Li H, Mitchell P, Rochtchina E, Burlutsky G, Wong TY, Wang JJ. Retinal vessel caliber and myopic retinopathy: the blue mountains eye study. Ophthalmic Epidemiol. 2011;18:275–80.
6. Azemin MZ, Daud NM, Ab Hamid F, Zahari I, Sapuan AH. Influence of refractive condition on retinal vasculature complexity in younger subjects. TheScientificWorldJournal. 2014;2014: 783525.
7. Kaneko Y, Moriyama M, Hirahara S, Ogura Y, Ohno-Matsui K. Areas of nonperfusion in peripheral retina of eyes with pathologic myopia detected by ultra-widefield fluorescein angiography. Investigative Ophthalmol Vis Sci. 2014;55:1432–9.
8. Yang Y, Wang J, Jiang H, Yang X, Feng L, Hu L, et al. Retinal microvasculature alteration in high myopia. Invest Ophthalmol Vis Sci. 2016;57:6020–30.
9. Li M, Yang Y, Jiang H, Gregori G, Roisman L, Zheng F, et al. Retinal microvascular network and microcirculation assessments in high myopia. Am J Ophthalmol. 2017;174:56–67.
10. Milani P, Montesano G, Rossetti L, Bergamini F, Pece A. Vessel density, retinal thickness, and choriocapillaris vascular flow in myopic eyes on OCT angiography. Graefe's Arch Clin Exp Ophthalmol = Albrecht von Graefes Arch fur klinische und experimentelle Ophthalmologie. 2018;256:1419–27.
11. Al-Sheikh M, Phasukkijwatana N, Dolz-Marco R, Rahimi M, Iafe NA, Freund KB, et al. Quantitative OCT angiography of the retinal microvasculature and the choriocapillaris in myopic eyes. Investig Ophthalmol Vis Sci. 2017;58:2063–69.
12. Fan H, Chen HY, Ma HJ, Chang Z, Yin HQ, Ng DS, et al. Reduced macular vascular density in myopic eyes. Chin Med J. 2017;130:445–51.
13. Cheng D, Chen Q, Wu Y, Yu X, Shen M, Zhuang X, et al. Deep perifoveal vessel density as an indicator of capillary loss in high myopia. Eye. 2019;33:1961–68.
14. Leng Y, Tam EK, Falavarjani KG, Tsui I. Effect of age and myopia on retinal microvasculature. Ophthalmic Surg Lasers Imaging Retin. 2018;49:925–31.
15. Mo J, Duan A, Chan S, Wang X, Wei W. Vascular flow density in pathological myopia: an optical coherence tomography angiography study. BMJ Open. 2017;7:e013571.
16. Yang S, Zhou M, Lu B, Zhang P, Zhao J, Kang M, et al. Quantification of macular vascular density using optical coherence tomography angiography and its relationship with retinal thickness in myopic eyes of young adults. J Ophthalmol. 2017;2017: 1397179.
17. Golebiewska J, Biala-Gosek K, Czeszyk A, Hautz W. Optical coherence tomography angiography of superficial retinal vessel density and foveal avascular zone in myopic children. PloS one. 2019;14:e0219785.
18. He J, Chen Q, Yin Y, Zhou H, Fan Y, Zhu J, et al. Association between retinal microvasculature and optic disc alterations in high myopia. Eye. 2019;33:1494–503.
19. Li Y, Miara H, Ouyang P, Jiang B. The comparison of regional RNFL and fundus vasculature by OCTA in Chinese myopia population. J Ophthalmol. 2018;2018:3490962.
20. Venkatesh R, Sinha S, Gangadharaiah D, Gadde SGK, Mohan A, Shetty R, et al. Retinal structural-vascular-functional relationship using optical coherence tomography and optical coherence tomography – angiography in myopia. Eye Vis. 2019;6:8.
21. Wang X, Kong X, Jiang C, Li M, Yu J, Sun X. Is the peripapillary retinal perfusion related to myopia in healthy eyes? A prospective comparative study. BMJ Open. 2016;6:e010791.
22. Wirth MA, Freiberg F, Pfau M, Wons J, Becker MD, Michels S. Optical coherence tomography angiography in age-related macular degeneration: persistence of vascular network in quiescent choroidal neovascularization. Acta Ophthalmol. 2017;95:428–30.
23. Takusagawa HL, Liu L, Ma KN, Jia Y, Gao SS, Zhang M, et al. Projection-resolved optical coherence tomography angiography of macular retinal circulation in glaucoma. Ophthalmology. 2017;124:1589–99.
24. Lee J, Rosen R. Optical coherence tomography angiography in diabetes. Curr Diabetes Rep. 2016;16:123.
25. Rosenfeld PJ, Durbin MK, Roisman L, Zheng F, Miller A, Robbins G, et al. ZEISS angioplex spectral domain optical coherence tomography angiography: technical aspects. Dev Ophthalmol. 2016;56:18–29.
26. Bennett AG, Rudnicka AR, Edgar DF. Improvements on Littmann's method of determining the size of retinal features by fundus photography. Graefe's Arch Clin Exp Ophthalmol = Albrecht von Graefes Arch fur klinische und experimentelle Ophthalmologie. 1994;232:361–7.
27. Knaapi L, Aarnisalo E, Vesti E, Leinonen MT. Clinical verification of the formula of Bennett et al. (1994) of determining the size of retinal features by fundus photography. Acta Ophthalmol. 2015;93:248–52.
28. Moghimi S, Hosseini H, Riddle J, Lee GY, Bitrian E, Giaconi J, et al. Measurement of optic disc size and rim area with spectral-domain OCT and scanning laser ophthalmoscopy. Investig Ophthalmol Vis Sci. 2012;53:4519–30.
29. Jiang H, Debuc DC, Rundek T, Lam BL, Wright CB, Shen M, et al. Automated segmentation and fractal analysis of high-resolution non-invasive capillary perfusion maps of the human retina. Microvasc Res. 2013;89:172–5.
30. Zhang M, Hwang TS, Campbell JP, Bailey ST, Wilson DJ, Huang D, et al. Projection-resolved optical coherence tomographic angiography. Biomed Opt Express. 2016;7:816–28.

31. Tan CS, Lim LW, Chow VS, Chay IW, Tan S, Cheong KX, et al. Optical coherence tomography angiography evaluation of the parafoveal vasculature and its relationship with ocular factors. Investig Ophthalmol Vis Sci. 2016;57:OCT224–34.

32. Shimada N, Ohno-Matsui K, Nishimuta A, Moriyama M, Yoshida T, Tokoro T, et al. Detection of paravascular lamellar holes and other paravascular abnormalities by optical coherence tomography in eyes with high myopia. Ophthalmology. 2008;115:708–17.

33. Sung MS, Lee TH, Heo H, Park SW. Association between optic nerve head deformation and retinal microvasculature in high myopia. Am J Ophthalmol. 2018;188:81–90.

34. Yousefi S, Qin J, Wang RK. Super-resolution spectral estimation of optical micro-angiography for quantifying blood flow within microcirculatory tissue beds in vivo. Biomed Opt Express. 2013;4:1214–28.

35. Zhou M, Lu B, Zhang P, Zhao J, Wang Q, Sun X. Determination of topographic variations in inner retinal blood flow areas in young Chinese subjects using optical coherence tomography angiography. Curr eye Res. 2017;42:1491–96.

36. Ohno-Matsui K. Proposed classification of posterior staphylomas based on analyses of eye shape by three-dimensional magnetic resonance imaging and wide-field fundus imaging. Ophthalmology. 2014;121:1798–809.

37. Man RE, Lamoureux EL, Taouk Y, Xie J, Sasongko MB, Best WJ, et al. Axial length, retinal function, and oxygen consumption: a potential mechanism for a lower risk of diabetic retinopathy in longer eyes. Investig Ophthalmol Vis Sci. 2013;54:7691–8.

38. Deng L, Gwiazda J, Manny RE, Scheiman M, Weissberg E, Fern KD, et al. Limited change in anisometropia and aniso-axial length over 13 years in myopic children enrolled in the correction of myopia evaluation trial. Investig Ophthalmol Vis Sci. 2014;55:2097–105.

39. Wei Y, Jiang H, Shi Y, Qu D, Gregori G, Zheng F, et al. Age-related alterations in the retinal microvasculature, microcirculation, and microstructure. Investig Ophthalmol Vis Sci. 2017;58:3804–17.

40. Faul F, Erdfelder E, Lang AG, Buchner A. G*Power 3: a flexible statistical power analysis program for the social, behavioral, and biomedical sciences. Behav Res Methods. 2007;39:175–91.